Acta Materialia 124 (2017) 59–70

Contents lists available at ScienceDirect

Acta Materialia

journal homepage: www.elsevier.com/locate/actamat

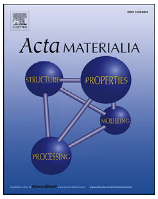

Full length article

Dislocation mediated variant selection for secondary twinning in compression of pure titanium

Shun Xu [a, b], Laszlo S. Toth [a, b, *], Christophe Schuman [a, b], Jean-Sébastien Lecomte [a, b],
Matthew R. Barnett [c]

[a] Laboratoire d'Etude des Microstructures et de Mécanique des Matériaux (LEM3), CNRS UMR 7239, Université de Lorraine, F-57045 Metz, France
[b] Laboratory of Excellence on Design of Alloy Metals for Low-mAss Structures (DAMAS), Université de Lorraine, France
[c] ARC Centre for Excellence for Design in Light Metals, Institute for Frontier Materials, Deakin University, Geelong, Australia

ARTICLE INFO

Article history:
Received 27 June 2016
Received in revised form
29 September 2016
Accepted 23 October 2016
Available online 4 November 2016

Keywords:
Titanium
EBSD
Twinning
Secondary twinning
Variant selection

ABSTRACT

By compression along the normal direction of rolled pure titanium sheet, primary $\{11\bar{2}2\}$ type compression twins were observed, followed by secondary $\{10\bar{1}2\}$ extension twins. The latter can be classified into three groups according to their misorientation with respect to the parent matrix grains: 41.34° around $<5\bar{1}\bar{4}3>$ (Group I), 48.44° around $<\bar{5}50\bar{3}>$ (Group II), and 87.85° around $<7\bar{4}\bar{3}0>$ (Group III). The experimental observations revealed the following activity frequency of these groups: Group II is the most frequent followed by Group I, and only a few secondary twins can be seen for Group III. When the classical Schmid factor (SF) analysis is applied, the smallest activity is predicted for Group III, in agreement with the experimental observations. However, the SF based criterion fails to distinguish between Group I and Group II variants. Similarly, the twin-shear accommodation based variant selection model proposed earlier for titanium [Qin and Jonas, Acta Mater. 75 (2014) 198–211] is not effective because the easiest accommodation by prismatic slips favors Group III variants which are nearly absent in the experiment. A possible explanation can be based on the smallest inclination angle of the secondary twinning habit plane with respect to the primary one, proposed by Barnett et al. [Acta Mater. 56 (2008) 5–15] which clearly favors Group II. It cannot make distinction between variants of the same group but can predict the right variants if complemented with the SF criterion. In the present work a new approach is proposed in order to disclose the preference for Group II variant over Group I. It is based on the special twinning geometry that applies to Group II; the intersection line of the primary and secondary twin planes lies in an active prismatic plane in the primary twin. Consequently, dislocation reactions are possible for the selection of secondary twin variant in Group II. Namely, prismatic <**a**> type dislocations in the primary twin can produce partial dislocations that activate the corresponding secondary twin variant. Nevertheless, a further selection rule has to be applied to choose one out of the two possible Group II variants; this is based on the higher Schmid factor of the two secondary variants. By contrast, pyramidal dislocations would be required for the formation of Group I twins, which is less likely due to their relatively high critical resolved shear stress.

1. Introduction

The wide application of hexagonal close packed (HCP) metals such as α-titanium, magnesium and zirconium in aerospace technology, automotive and nuclear industry requires a deep understanding of their deformation mechanisms. These metals are characterized by a large variety of possible slip systems [1–3]: basal <**a**> $\{0002\}<11\bar{2}0>$, prismatic <**a**> $\left\{1\bar{1}00\right\}<11\bar{2}0>$, pyramidal ⟨**c**+**a**⟩ $\{10\bar{1}1\}<11\bar{2}3>$, and pyramidal <**a**> $\left\{1\bar{1}01\right\}<11\bar{2}0>$. Besides slip, deformation twinning plays a significant role in the plastic deformation to accommodate the strain along c-axis of the crystal, especially at low temperatures [4] and high strain rates [5]. At room temperature, several twinning modes have been observed in α-titanium [6]. Extension twins including $\{10\bar{1}2\}<\bar{1}011>$,

---

[*] Corresponding author. Laboratoire d'Etude des Microstructures et de Mécanique des Matériaux (LEM3), CNRS UMR 7239, Université de Lorraine, F-57045 Metz, France.

E-mail address: laszlo.toth@univ-lorraine.fr (L.S. Toth).

http://dx.doi.org/10.1016/j.actamat.2016.10.063
1359-6454/

$\{11\bar{2}1\}<\overline{11}26>$ and $\{11\bar{2}3\}<\overline{11}22>$ induce a positive strain along the c-axis of the parent grain, while contraction twins, such as $\{11\bar{2}2\}<11\overline{23}>$, $\{11\bar{2}4\}<22\overline{43}>$ and $\{10\bar{1}1\}<10\overline{12}>$, cause reduction along the c-axis [7].

The large reorientation caused by primary twinning can reposition initially non-active twinning systems of the parent grain into more favorable orientation, promoting secondary twinning inside the primary twins. The following secondary twin systems are reported in magnesium alloys: $\{10\bar{1}2\}$ twins in $\{10\bar{1}1\}$ primary twins [8–10], and $\{10\bar{1}2\}$ twins in primary $\{10\bar{1}2\}$ twins [11,12]. The former can readily appear during uniaxial deformations [13,14]. Barnett et al. [8] reported that the $\{10\bar{1}1\}-\{10\bar{1}2\}$ double twin variants that are favored are those that correspond to minimum compatibility strain in the primary $\{10\bar{1}1\}$ twins. Martin et al. [9] found that the secondary twin variants having the greatest potential for growth and with the highest resolved shear stress are most favorable during the selection of secondary twin variants. $\{10\bar{1}2\}-\{10\bar{1}2\}$ double twins were found in AZ31 in uniaxial deformation at 77 K, possibly due to the absence of non-basal slip at low temperature, while they did not appear at room temperature deformation where non-basal slip can take place [11]. Wang et al. [15–17] declared nucleation mechanism of twinning in HCP metals by using simulation. Beyerlein et al. rationale selection based on nucleation via dislocation reaction at the primary twin interface [18]. In pure titanium, $\{11\bar{2}2\}$ and $\{10\bar{1}2\}$ twins are most frequently observed at room temperature [6,19,20], compared to other twinning systems. Christian and Mahajan put forward that a low shear and a small shuffling facilitates the formation of these twins [4]. Several compression tests were carried out on commercially pure titanium to study secondary $\{10\bar{1}2\}$ extension twinning inside primary $\{11\bar{2}2\}$ compression twins in Refs. [21–23]. Jonas et al. [10,23,24] recently employed strain accommodation to evaluate the selection of twin variants. In their work, the generation of secondary twins was explained by inspecting several deformation modes in the adjacent parent grains to accommodate the shear induced by the secondary twins [23]. It was proposed that those secondary twin variants are initiated for which the strain can be accommodated the most easily by prismatic or basal glide in the parent. The displacement gradient tensor of the shear operating in the secondary twin frame was transformed into the crystal fame of the neighboring parent grain to identify the slip system in the parent grain that can accommodate the twinning shear displacement in the twin boundary region. Wang et al. [25,26] considered twinning accommodated by twinning on the other side of a boundary. They employed the Luster-Morris parameter [26–28] defined by $m' = \cos\psi \bullet \cos\kappa$, where ψ is the angle between the normal of the two planes and κ is the angle between two shear directions of the systems, which can be used to quantify the compatibility of accommodating slip or twinning. Recently, the preferred secondary twins were found with a misorientation relation of 41° around a $<5\overline{143}>$ axis compared to the matrix in commercially pure titanium subjected to cold-rolling [29]. The activation of secondary twinning induced by channel-die compression was recently reported and found to be reasonably consistent with a simplified Schmid factor (SF) criterion [30].

There are evidently a range of findings and interpretations in the literature and the present work aims to test their applicability to secondary $\{10\bar{1}2\}$ twining within primary $\{11\bar{2}2\}$ twins in uniaxially compressed pure titanium. It is found in the present work that the only SF based and also the accommodation based secondary twin selection criteria [23] cannot explain the experimental observations. However, the habit plane orientation based criterion - originally proposed for magnesium [8] - applies also to titanium; i.e., it selects the right group (Group II). It does not, however, select the right variant within the group. The main contribution to the topic in the present work is a new criterion which is also able to reproduce the experimental secondary twinning activity. It is based on the special geometry that applies to Group II secondary twins in titanium: there is a common intersection line between three planes: the active prismatic plane in the primary twin and the primary and secondary twin planes. This special geometry makes possible dislocation reactions that are necessary for producing the partial dislocations of the secondary twin. Nevertheless, the Schmid factor criterion is still needed to choose between the two possible Group II $\{10\bar{1}2\}$ twin variants inside the $\{11\bar{2}2\}$ primary twins.

2. Experimental procedure

In the current study, the material used was rolled commercially pure titanium T40 sheet (ASTM grade 2) with a thickness of 1.5 mm. The composition is given in Table 1. It is generally understood that deformation twinning is more active with a larger grain size [31–33]. Therefore, samples with a large grain size were prepared by annealing in a vacuum furnace at 800 °C for 2 h, leading to a fully-recrystallized microstructure. By using a Zwick 120T machine, the samples were deformed at room temperature with 8.1% reduction at a strain rate of $1 \times 10^{-3}\ s^{-1}$. The compression direction (CD) was parallel to ND (normal direction). After compression, the rolling plane of the compressed sample was ground with SiC papers of grits from $1200^{\#}$ to $4000^{\#}$. Finally, electrolytic polishing was conducted at 35 V and 5 °C for 5 s in a solution of 10% perchloric acid and 90% methanol.

Electron backscatter diffraction (EBSD) measurements were performed on a JEOL 6500F field emission gun (FEG) and on a JSM 6490 SEM microscope equipped with an EBSD camera and the AZtec acquisition software package (Oxford Instruments). The sample was tilt by an angle of 70°. A voltage of 20 kV was used with a working distance of 15 mm. A step size of 5 μm was adopted to detect the texture of the initial material. For more detailed examination of twins, EBSD patterns were acquired on the deformed sample at a step size of 0.5 μm. The texture was analysed with the help of the JTEX software [34] and presented in pole figures.

Crystal plasticity simulations were carried out to obtain information on the required slip systems for accommodating the twin shears that are produced by the secondary twins at primary twin boundary in the parent grain. The fully imposed Taylor approach is suitable for such calculation in which the twin shear is imposed on the parent orientation. The approach based on rate sensitive slip proposed in Ref. [35] was used for this purpose. The results are reported in Section 4.2.

3. Results

3.1. Microstructure in the initial and deformed states

Fig. 1 presents the microstructure of the initial material in form of EBSD inverse pole figure (IPF) where the ND axis was projected with the shown color code. The material was fully recrystallized with an average grain size of ~160 μm and presented no twins. RD and TD represent the rolling and transverse directions, respectively.

Table 1
Chemical composition of the commercially-pure titanium T40 used in the study.

Element	H	C	N	O	Fe	Ti
Composition (wt. ppm)	3	52	41	1062	237	Balance